# A Stable and Cost-Effective Anode Catalyst Structure for Formic Acid Fuel Cells**

*Sunghyun Uhm, Hye Jin Lee, Youngkook Kwon, and Jaeyoung Lee*

The high energy density, fast oxidation kinetics, and convenience of use of liquid formic acid (HCOOH), as well as the simplicity of power-system integration make direct formic acid fuel cells (DFAFCs) a promising power source for portable device applications.[1–3] Considerable progress in aspects of DFAFC research and engineering has been achieved in recent years, which has enabled the fuel-cell technology to be implemented in practical devices. However, large-scale practical commercialization has been limited by several challenging issues such as high anode overpotential, excessive fuel and water permeability of the polymer electrolyte membrane, and questionable long-term durability of the fuel cells.

The issue of high overpotential for anode catalysts is associated with the formation of poisons on the catalyst surface and also with the large amount of catalyst loading. To date, despite the problem of being strongly poisoned by intermediate species, Pt is the best-known anode catalyst for the oxidation of small organic molecules.[4,5] Besides Pt, Pd catalysts have recently shown superior performances compared to platinum-based catalysts in the oxidation ultrapure HCOOH in DFAFCs, because of the great initial activity of Pd, even at low temperature.[5–7] However, Pd catalysts have a significant drawback; their high performance is not sustained for extended time periods, largely because of the vulnerability of these catalysts towards uncharacterized intermediate species[8–10] and the potential for the dissolution of Pd in acidic solutions.[11,12]

To enhance the power performance as well as the durability of the catalyst, we have recently demonstrated that irreversible modification of the Pt metal surface with foreign metal adatoms such as Bi,[3,13,14] Pb[15], and Sb[14,16] is a powerful method to drive a practical DFAFC system. In addition, an effective anode structure that alleviates mass

transport of HCOOH in the membrane electrode assembly (MEA) enabled us to reduce the amount of Pt loading and extend the range of the HCOOH concentration windows.[17] Herein, we report a novel approach for the fabrication of more stable and cost-effective anode catalysts for DFAFC by using a three-step electrochemical process. The newly developed catalyst, which contains Pt modified with Bi, is directly applied to the fuel cell to evaluate its catalytic activity and performance.

The PtBi catalyst was fabricated in three consecutive electrochemical steps, namely: 1) electrochemical oxidation of carbon paper to form the adequate catalyst support, followed by 2) Pt electrodeposition, and 3) underpotential deposition (UPD) of Bi onto the Pt. The conceptual design of the final electrode is illustrated schematically in Figure 1 and
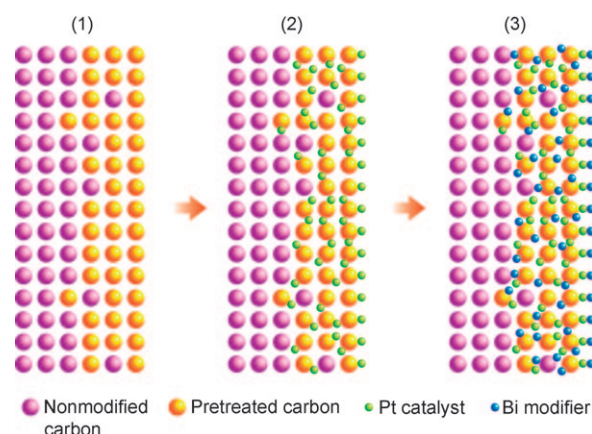


*Figure 1.* Schematic representation showing the electrode structure of PtBi anode catalysts fabricated by using a three-step electrochemical procedure, after electrochemical oxidation of carbon paper electrodes to form the adequate catalyst support (1), subsequent Pt electrodeposition (2), and subsequent underpotential deposition of Bi onto the as-prepared Pt catalyst (3).

each individual step of which was independently characterized in previous studies.[3,18,19] Commercially available plain carbon paper was used to provide an ideal percolation network because of its ideal structure. A controlled electrochemical oxidation of plain carbon paper led to a thin, well-dispersed catalyst layer at the outermost part of the carbon paper (Figure 1).

The activity of anode catalysts in fuel cell applications is critically affected by their structure, surface morphology, surface coverage, and durability. The catalysts were fully characterized after each electrochemical step to provide a clear structure–property relationship with respect to the

[*] Dr. S. Uhm, Y. Kwon, Prof. Dr. J. Lee
Electrochemical Reaction & Technology Laboratory (ERTL)
Department of Environmental Science and Engineering
Gwangju Institute of Science and Technology (GIST)
261 Cheomdan-gwagiro, Gwangju 500-712 (South Korea)
Fax: (+82) 629702434
E-mail: jaeyoung@gist.ac.kr
Homepage: http://env1.gist.ac.kr/ertl

Prof. H. J. Lee
Department of Chemistry, Kyungpook National University
1370 Sankyuk-dong, Daegu 702-701 (South Korea)

above properties by using X-ray photoelectron spectroscopy (XPS), field emission scanning electron microscopy (HR-SEM), X-ray diffraction (XRD), and cyclic voltammetry (CV). Figure 2 shows XPS spectra (Figure 2a,b) of carbon
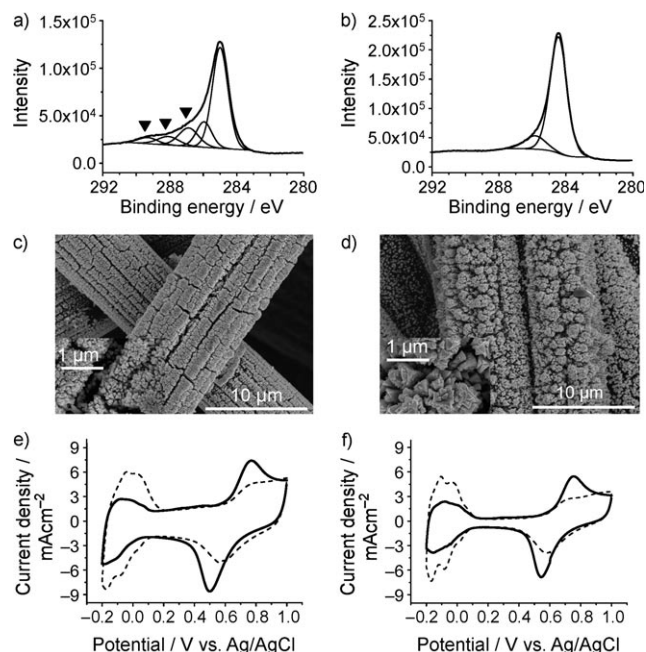


***Figure 2.*** Deconvoluted C1s peaks region from XPS analysis of a) Ec-Ox and b) As-Re carbon paper. Representative SEM images (5000×) of electrodeposited Pt (0.5 mg cm$^{-2}$) on the corresponding carbon papers. c) Ec-Ox carbon paper and d) As-Re carbon paper. The insets show more highly magnified images (50000×) of each nanoparticle. Electrochemical measurements of Pt (dotted line) and PtBi (solid line) catalyst on e) Ec-Ox and f) As-Re carbon paper in HClO$_4$ (0.5 M) at a scan rate of 50 mV s$^{-1}$ at room temperature.

paper before (as-received, As-Re) and after electrochemical oxidation (Ec-Ox), SEM images (Figure 2c,d) of electrodeposited Pt on the corresponding carbon paper, and cyclic voltammograms (Figure 2e,f) before and after Bi UPD on the corresponding Pt catalysts. The electrochemical oxidation enriched the oxygen-containing species on the carbon paper (Ec-Ox) surface (Figure 2a, ▼), which showed a capacitance at least five times higher than that of the As-Re carbon paper (see Figure S1 in the Supporting Information), and led to the formation of more-dispersed Pt particles (Figure 2c);[20] this arises from an increase in surface accessibility, as oxygen-containing species on the carbon surface act as acidic sites for the adsorption of the catalyst precursors.[21,22] The average particle size of electrodeposited Pt as obtained by XRD (see Figure S2 in the Supporting Information) and the Debye–Scherrer formula was $(15 \pm 2)$ nm on Ec-Ox and $(21 \pm 3)$ nm on As-Re carbon paper. Usually, the electrodeposited Pt particle size falls in the range of 20–70 nm unless the Pt loading is ultralow (less than 0.05 mg cm$^{-2}$).[23,24] The particle-size measurements indicate that the Pt particles synthesized on Ec-Ox carbon paper are well-dispersed and relatively

small despite having an amount of Pt that is ten times higher (0.5 mg cm$^{-2}$) than the ultralow loading.

After having confirmed the increased functionality and the high dispersion of the Pt particles, electrochemical measurements were carried out to evaluate the surface coverage and stability of adsorbed Bi on the Pt catalyst (Figure 2e,f). It is clear that the presence of irreversibly adsorbed Bi atoms on Pt electrodes causes a decrease of the hydrogen adsorption/desorption charge in the potential range below 0.1 V. The presence of the adatom on the surface can be also monitored by the redox process that takes place at potentials higher than approximately 0.4 V (shown as solid lines in Figure 2e,f). The stability of the voltammetric profile upon cycling in the chosen potential window reflects the irreversible adsorption of Bi on the Pt substrate. Moreover, the adatom coverage calculated by the hydrogen adsorption/desorption charge before and after Bi UPD shows that, while the charges of hydrogen on Pt (regardless of the electrochemical oxidation of the carbon paper support) are almost identical before Bi UPD, the hydrogen desorption charge value of the Ec-Ox carbon paper after Bi UPD becomes much smaller than that of As-Re carbon paper (see Table S1 in the Supporting Information). In particular, the hydrogen desorption charge for the Ec-Ox carbon paper is significantly decreased. The increase of the Bi surface coverage could be attributed to the increase in irreversibility that results from the increase of the double layer region (see Figure S1 in the Supporting Information) as well as the smaller particle size of electrodeposited Pt on the Ec-Ox carbon paper.[25] Under the given conditions, the increase of Bi surface coverage can enhance the electrooxidation of HCOOH, especially at adatom coverages less than 80%.[26,27]

The final criterion for the preparation of catalysts is their successful application as electrodes in an actual fuel cell system that consists of polymer membranes (MEAs). Current–voltage polarization curves obtained using an MEA prepared with two different anode PtBi catalysts placed on Ec-Ox and As-Re carbon paper are shown in Figure 3. Around 0.5 V, where an activation polarization dominates the activity of the catalyst, the current density of the PtBi catalyst
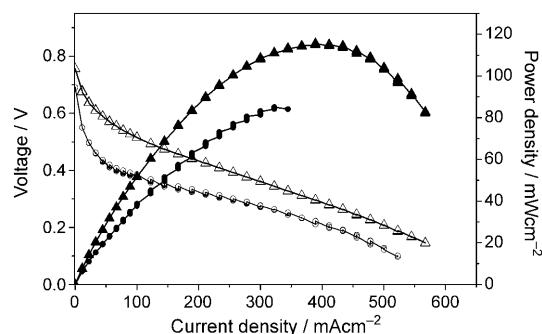


***Figure 3.*** Measurements of two MEAs prepared with PtBi anode catalysts: current–voltage polarization curves for Ec-Ox (△) and As-Re (○) carbon paper and current–power density for Ec-Ox (▲) and As-Re (●) carbon paper. The fuel cells were operated at 60°C with formic acid (6 M) as the fuel and dry air as an oxidant. The catalyst loading was 0.5 mg cm$^{-2}$.

on Ec-Ox carbon paper is about four times higher than that of PtBi on As-Re carbon paper, together with higher open-circuit voltage. This behavior is attributed to more effective formation and growth of the electrodeposited Pt catalyst (see the SEM images in Figure 2) and consequently a higher coverage of UPD Bi. Such an enhanced performance indicates that use of a PtBi catalyst on Ec-Ox carbon paper can lead to a substantial reduction of the required amount of Pt in a DFAFC. In fact, the amount of Pt in this study, 0.5 mg cm$^{-2}$, was only 10–20% of that of a typical commercial catalyst.[1–3] Additionally, the Bi coverage does not influence the power performance any more over 67% coverage under given conditions (Figure S3 in the Supporting Information).

A final question is whether PtBi or conventional catalysts such as Pd or PtRu black is more effective in a DFAFC under the given operating conditions. A comparison between these catalysts, each with a metal loading of 3 mg cm$^{-2}$, is shown in Figure 4 for both current–voltage polarization measurements and voltage variation acquired as a function of time at a constant current density. Our PtBi catalyst shows a lower catalytic performance than that of the Pd catalyst (Figure 4a). However, the PtBi catalyst outperforms the Pd black catalyst if the currents are normalized by the total weight of the precious metal (Figure 4b), and the performance of the Pd catalyst decreases gradually not only during polarization measurements but also during constant current measurements (Figure 4c). On the other hand, the PtBi catalyst shows a very stable performance although the initial voltage is relatively low compared to the Pd catalyst. This is mainly attributed to partial oxidation of Bi on the Pt electrode, as the oxidized forms of Bi are not effective for electrooxidation of HCOOH. Note that the deposition of Bi should be reversible enough to sustain the enhanced performance.

A platinum-based anode catalyst (PtBi) that can be cost effectively and more robustly used in formic acid fuel cells has been developed. The well-dispersed PtBi catalysts, which are prepared in three electrochemical steps, possess both a higher degree of dispersion of electrodeposited Pt and a significantly higher Bi adatom coverage. A significantly enhanced power performance with Pt loading of only 0.5 mg cm$^{-2}$ in a fuel cell operation was also achieved. Furthermore, in comparison with commercial Pd catalysts, the PtBi catalyst described herein is not only more robust but also cost-effective because of its long-term durability and ultralow Pt loading. It is expected that extensive efforts will be made in the near future in fuel cell research to improve the surface density of commercial catalysts as well as the reduction of their Pt content, together with extending the lifetimes of anode catalysts. One promising method could be the development of advanced carbon materials as catalyst supports as well as the optimization of ionomer content in the catalyst layer with regard to corresponding carbon materials.

## Experimental Section

Carbon paper (TGPH-060, E-TEK) was used as catalyst support. For the electrochemically oxidized carbon paper electrodes (Ec-Ox), a constant potential of 2.0 V was applied in HClO$_4$ (0.5 M) for 2 min with a potentiostat (Autolab PGSTAT30) using an Ag/AgCl reference
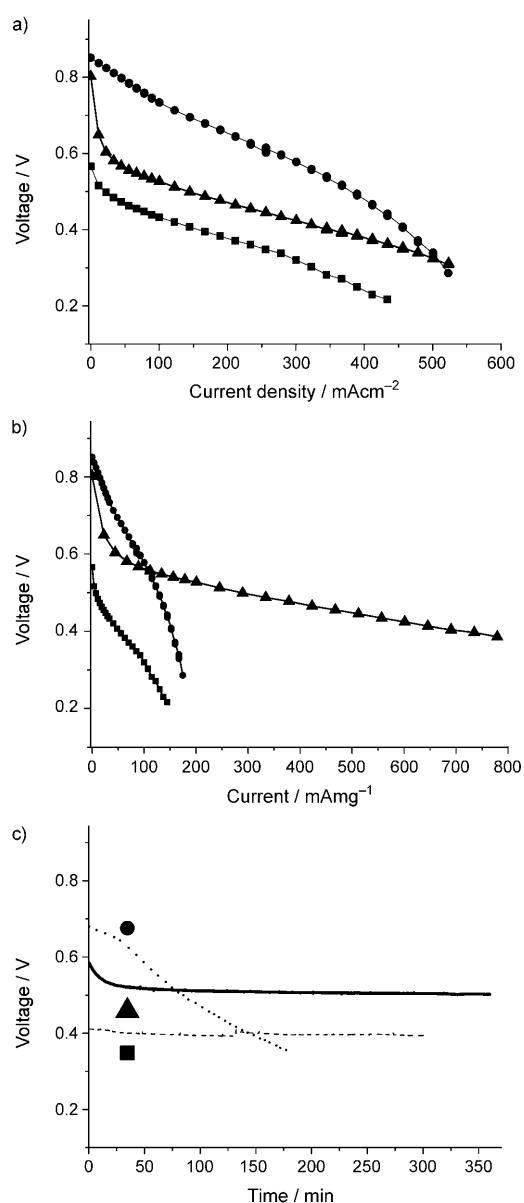


*Figure 4.* Current–voltage polarization measurements for direct formic acid fuel cells with different anode catalysts (▲ PtBi, ● Pd, ■ PtRu). Currents are normalized by geometric area (a) and total weight of the respective precious metals (b). Voltage variation as a function of time at a constant current density of 150 mA cm$^{-2}$ (c). The fuel cell was operated at 60 °C with formic acid (6 M) as the fuel and dry air as an oxidant.

electrode and a platinized Pt counterelectrode. Following the electrochemical oxidation process, Pt was electrodeposited on Ec-Ox and As-Re carbon paper in H$_2$PtCl$_6$ (10 mM, Sigma), Pb-(CH$_3$COO)$_2$ (0.2 mM, Junsei), and HClO$_4$ (0.1 M, Aldrich). Depositions were carried out at 0 V and the amount of deposited metal was controlled by the total charge applied and its current efficiency is 46–50%. For the PtBi UPD, Bi$_2$O$_3$ (1–5 mM) was first added to HClO$_4$ solution (0.1 M) and was conducted at 0.0 or 0.3 V to control the homogeneous surface coverage of Bi, depending on the apparent OCV, for 10 min. CVs were recorded at 50 mV s$^{-1}$ in HClO$_4$ (0.5 M).

Structural analysis of Pt was carried out using XRD (D/MAX Ultima III diffractometer), and the surface morphology was characterized with a FE-SEM (Hitachi S-4700). The composition and

# Communications

electronic state of the surface region was analyzed using XPS (VG Multilab 2000).

Preparation of MEAs:[3,17,28] the anode consisted of PtBi ($0.5 \text{ mg cm}^{-2}$), commercial Pd black ($3.0 \text{ mg cm}^{-2}$, Aldrich), or PtRu black ($3.0 \text{ mg cm}^{-2}$, Johnson Matthey), impregnated with Nafion solution (Aldrich, 5 wt %). The ionomer content in the catalyst layer was optimized with respect to metal loading ranging from 0.3 to $1.0 \text{ mg cm}^{-2}$. The cathode consisted of carbon paper as substrate (SGL 35BC) on which Pt black ($3.0 \text{ mg cm}^{-2}$, Johnson Matthey) and ionomers ($0.3 \text{ mg cm}^{-2}$ content) were loaded. The MEA structure and the experimental details of polarization curves and durability tests are reported elsewhere[3,17,28] (see also Figure S4 in the Supporting Information).

[1] S. Ha, R. Larsen, Y. Zhu, R. I. Masel, *Fuel Cells* **2004**, *4*, 337.
[2] S. Ha, Z. Dunbar, R. I. Masel, *J. Power Sources* **2006**, *158*, 129.
[3] S. Kang, J. Lee, J. K. Lee, S.-Y. Chung, Y. Tak, *J. Phys. Chem. B* **2006**, *110*, 7270.
[4] Y. X. Chen, M. Heinen, Z. Jusys, R. J. Behm, *Angew. Chem.* **2006**, *118*, 995; *Angew. Chem. Int. Ed.* **2006**, *45*, 981.
[5] S. E. Habas, H. Lee, V. Radmilovic, G. A. Somorjai, P. Yang, *Nat. Mater.* **2007**, *6*, 692.
[6] W. P. Zhou, A. Lewera, R. Larsen, R. I. Masel, P. S. Bagus, A. Wieckowski, *J. Phys. Chem. B* **2006**, *110*, 13393.
[7] N. Hoshi, K. Kida, M. Nakamura, M. Nakada, K. Osada, *J. Phys. Chem. B* **2006**, *110*, 12480.
[8] M. J. Llorca, J. M. Feliu, A. Aldaz, J. Clavilier, *J. Electroanal. Chem.* **1994**, *376*, 151.
[9] M. Baldauf, D. M. Kolb, *J. Phys. Chem.* **1996**, *100*, 11375.
[10] P. K. Babu, H. S. Kim, J. H. Chung, E. Oldfield, A. Wieckowski, *J. Phys. Chem. B* **2004**, *108*, 20228.
[11] F. R. Hartley in *Chemistry of the Platinum Group Metals* (Ed.: F. R. Hartley), Elsevier, New York, **1991**, chap. 1.
[12] J. Sollon-Gullón, V. Montiel, A. Aldaz, J. Clavilier, *Electrochem. Commun.* **2002**, *4*, 716.
[13] E. Casado-Rivera, Z. Gal, A. C. D. Angelo, C. Lind, F. J. DiSalvo, H. D. Abruna, *ChemPhysChem* **2003**, *4*, 193.
[14] E. Casado-Rivera, D. J. Volpe, L. Alden, C. Lind, C. Downie, T. Vazquez-Alvarez, A. C. D. Angelo, F. J. DiSalvo, H. D. Abruna, *J. Am. Chem. Soc.* **2004**, *126*, 4043.
[15] S. Uhm, S. T. Chung, J. Lee, *Electrochem. Commun.* **2007**, *9*, 2027.
[16] J. K. Lee, H. Jeon, S. Uhm, J. Lee, *Electrochim. Acta* **2008**, *53*, 6089.
[17] S. Uhm, Y. Kwon, S. T. Chung, J. Lee, *Electrochim. Acta* **2008**, *53*, 5162.
[18] I. D. Harry, B. Saha, I. W. Cumming, *J. Colloid Interface Sci.* **2006**, *304*, 9.
[19] S. Domínguez-Domínguez, J. Arias-Pardilla, Á. Berenguer-Murcia, E. Morallón, D. Cazorla-Amorós, *J. Appl. Electrochem.* **2008**, *38*, 259.
[20] A. Wieckowski, E. R. Savinova, C. G. Vayenas, *Catalysis and Electrocatalysis at Nanoparticle Surfaces*; Marcel Dekker, New York, **2003**.
[21] M. Watanabe, H. Sei, P. Stonehart, *J. Electroanal. Chem.* **1989**, *261*, 375.
[22] M. A. Fraga, E. Jordao, M. J. Mendes, M. M. A. Freitas, J. H. Faria, J. L. Figueiredo, *J. Catal.* **2002**, *209*, 355.
[23] H. Tang, J. H. Chen, Z. P. Huang, D. Z. Wang, Z. F. Ren, L. H. Nie, Y. F. Kuang, S. Z. Yao, *Carbon* **2004**, *42*, 191.
[24] Y. Y. Shao, G. P. Yin, J. J. Wang, Y. Z. Gao, P. F. Shi, *J. Electrochem. Soc.* **2006**, *153*, A1261.
[25] C. Rice, Y. Tong, E. Oldfield, A. Wieckowski, *Electrochim. Acta* **1998**, *43*, 2825.
[26] J. Clavilier, A. Fernández-Vega, J. M. Feliu, A. Aldaz, *J. Electroanal. Chem.* **1989**, *258*, 89.
[27] E. Leiva, T. Iwasita, E. Herrero, J. M. Feliu, *Langmuir* **1997**, *13*, 6287.
[28] S. Uhm, T. Noh, Y. D. Kim, J. Lee, *ChemPhysChem* **2008**, *9*, 1425.